



Can fully iterative reconstruction technique enable routine abdominal CT at less than 1 mSv?

Azadeh Tabari^a, Ramandeep Singh^{a,*}, Ruhani Doda Khera^a, Yiemeng Hoi^b, Erin Angel^b, Mannudeep K. Kalra^a, Rachna Madan^c

^a MGH Webster Center for Quality and Safety, Department of Radiology, Massachusetts General Hospital and Harvard Medical School, Boston, Massachusetts, USA

^b Canon Medical Systems USA, Inc., Tustin, California, USA

^c Department of Radiology, Brigham and Women's Hospital and Harvard Medical School, Boston, Massachusetts, USA

ARTICLE INFO

Keywords:

Iterative reconstruction
Forward projected model-based
Filtered back projection
Sub-milli-Sievert
Radiation dose
CT abdomen

ABSTRACT

Objective: We assessed the effect of the forward projected model-based reconstruction technique (FIRST) on lesion detection of routine abdomen CT at < 1 mSv.

Materials and methods: Thirty-seven adult patients gave written informed consent for acquisition of low-dose CT (LDCT) immediately after their clinically-indicated, standard of care dose (SDCT), routine abdomen CT on a 640-slice MDCT (Aquillion One, Canon Medical System). The LDCT series were reconstructed with FIRST (at STD (Standard) and STR (Strong) levels), and SDCT series with filtered back projection (FBP). Two radiologists assessed lesions in LD-FBP and FIRST images followed by SDCT images. Then, SDCT and LDCT were compared for presence of artifacts in a randomized and blinded fashion. Patient demographics, size and radiation dose descriptors (CTDIvol, DLP) were recorded. Descriptive statistics and inter-observer variability were calculated for data analysis.

Results: Mean CTDIvol for SDCT and LDCT were 13 ± 4.7 mGy and 2.2 ± 0.8 mGy, respectively. There were 46 true positive lesions detected on SDCT. Radiologists detected 38/46 lesions on LD-FIRST-STD compared to 26/46 lesions on LD-FIRST-STR. The eight lesions (liver and kidney cysts, pancreatic lesions, sub-cm peritoneal lymph node) missed on LD-FIRST-STD were seen in patients with BMI > 25.8 kg/m². Diagnostic confidence for lesion assessment was optimal in LD-FIRST-STD setting in most patients regardless of their size. The inter-observer agreement (kappa-value) for overall image quality were 0.98 and 0.84 for LD-FIRST-STD and STR levels, respectively.

Conclusion: FIRST enabled optimal lesion detection in routine abdomen CT at less than 1 mSv radiation dose in patients with body mass less than ≤ 25.8 kg/m².

1. Introduction

With increasing use of CT in modern medical practice, concerns have been raised over the associated radiation doses. CT vendors have introduced hardware technologies and image reconstruction methods to enable radiation dose optimization while maintaining an acceptable level of diagnostic quality. With the conventional filtered back projection and image-based iterative reconstruction methods, a decrease in CT radiation dose can impair the diagnostic confidence particularly for evaluation of low contrast organs or lesions such as in the abdomen and brain. Although a “smoother” or “softer” reconstruction kernels reduce the image noise in low dose CT, they impair spatial resolution [1].

Iterative reconstruction (IR) techniques for reconstructing CT images were described soon after the invention of CT scanners, as early as in 1973, but their application was hampered due to slow and low computational power [2]. With improvements in the computation power and speed, thanks to the video gaming industry, most CT vendors introduced commercial IR techniques to enable radiation dose reduction without sacrificing diagnostic confidence compared to the conventional filtered back projection techniques [3,4].

IR techniques can be classified into the hybrid IR (HIR) and the model-based IR (MBIR) techniques [1,5]. The MBIR employs models for image acquisition, statistics, and system geometry, whereas the HIR combines the analytical and iterative approaches to reduce the image

* Corresponding author at: MGH Webster Center for Quality and Safety, Department of Radiology, Massachusetts General Hospital and Harvard Medical School, 75 Blossom Court, Suite 236, Boston, MA 02114, USA.

E-mail address: rsingh17@mgh.harvard.edu (S. Ramandeep).

<https://doi.org/10.1016/j.ejro.2019.05.001>

Received 6 February 2019; Received in revised form 15 April 2019; Accepted 13 May 2019

Available online 21 June 2019

2352-0477/ © 2019 The Authors. Published by Elsevier Ltd. This is an open access article under the CC BY-NC-ND license

(<http://creativecommons.org/licenses/by-nc-nd/4.0/>).

noise [6]. Most CT vendors have developed diverse IR approaches. GE Healthcare (Waukesha, Wis.) introduced HIR named adaptive statistical IR (ASiR) in the year 2008. In the same year, Siemens Healthineers (Forchheim, Germany) commercialized HIR called image reconstruction in image space (IRIS) [4,7]. At about the same time, iDose (Philips Healthcare, Best, The Netherlands) and adaptive iterative dose reduction (AIDR-3D, Canon Medical Systems Corporation, Tochigi, Japan) were introduced [3,8]. In subsequent years, other IR methods were introduced including Veo and ASiR V (GE Healthcare), Safire and Admire (Siemens), IMR (Philips) and FIRST (Canon) [9–11].

The recently introduced Forward projected model-based Iterative Reconstruction SoluTion (FIRST) deploys a three-dimensional (3D) image reconstruction approach based on a forward and statistical model in the projection data to enhance the spatial resolution and reduce the image noise [12]. Compared to AIDR-3D, the FIRST optimizes image quality jointly in sinogram and image spaces [13]. The FIRST images are subjected to a regularization step to adapt the images based on organ specificity such as for abdomen, heart, lung, and bone. These features are then combined and undergo several iterations before converging to a final image. To our best knowledge, prior studies have not assessed the FIRST for enabling sub-milli-Sievert abdomen CT [14]. We hypothesized that FIRST can enable radiation dose reduction while maintaining diagnostic confidence in low radiation dose abdomen CT. To test this hypothesis, we assessed the effect of the FIRST on lesion detection in routine abdomen CT performed at low dose (LDCT at < 1 mSv).

2. Material and methods

2.1. Approvals and disclosures

The Human Research Committee of the Institutional Review Board approved our prospective multi-institutional study. The study was compliant with the Health Insurance Portability and Accountability Act (HIPAA). A study coauthor, MKK received research grants from Canon Medical Systems USA, Inc. and Siemens Healthineers. YH and EA are employees of Canon Medical Systems USA, Inc. All study coauthors had unrestricted access to the study data and the manuscript.

2.2. Patients

We prospectively enrolled 37 consecutive adult patients (17 women and 20 men; mean age = 63 ± 14 years) undergoing routine contrast-enhanced abdomen CT examinations for clinically indicated reasons. The most common clinical indications were abdominal pain, cancer diagnosis and staging, and unexplained loss of weight. All participating patients gave written informed consent after understanding the risks associated with additional radiation dose. All patients met the following inclusion criteria: hemodynamic stability, age > 56 years, body mass index (BMI) ≤ 32 kg/m², understand English, ability to follow breath-hold instructions, and hold breath for at least 5 s. We excluded patients undergoing urgent CT, patients with hemodynamic instability, shortness of breath, and inability to understand or follow scan instructions from the study. We recorded weight and height of all patients to estimate their body mass index (BMI).

2.3. Scanning techniques

All patients underwent standard-of-care routine abdomen CT (SDCT) in a supine position on a 640-slice multidetector-row CT scanner (Aquilion One, Canon Medical System Corporation). Patient's arms were placed over their head as per the standard of care procedure. After positioning the patients on the scan table, anteroposterior and lateral planning radiographs were acquired at 120 kV and 20 mA. To avoid motion related artifacts, patients were instructed to avoid any voluntary motion and follow breath-hold instruction for both SDCT and

LDCT acquisitions.

The scan parameters for SDCT included helical scan mode, 80 x 0.5 mm detector configuration, 0.5-second gantry rotation time, beam pitch of 0.9–1.1:1, 120 kV, and automatic exposure control (SureExposure 3D, Canon Medical System Corporation). Scan length extended from the top of the diaphragm to the pubic symphysis. All patients received 80–100 mL of intravenous non-ionic iodinated contrast agent (Iopamidol 370 mg%, Bracco Diagnostics, Princeton, NJ) at a rate of 2–3 mL/s via antecubital vein. Scanning was initiated at a fixed delay of 60 s to obtain images in the portal venous phase.

All scan parameters with exception of tube current and scan length were kept identical between the LDCT and SDCT acquisitions. LDCT images were acquired through the upper abdomen from the top of the liver to its inferior tip. As opposed to the SDCT, we used fixed tube current so that additional dose length product (DLP) from the research LDCT images was less than 65 mGy.cm (to maintain an estimated effective dose < 1 mSv). Thus, most CT exams were performed between 30–50 mA s to attain DLP of 65 mGy.cm for LDCT images. Use of fixed tube current for acquiring LDCT has been reported in prior publications as well [15,16]. Both CT Dose Index volume (CTDIvol) and DLP were recorded for all SDCT and LDCT image series. We planned the acquisition of the LDCT image series before acquiring SDCT so that the time interval between the LDCT and SDCT series was less than 5–10 seconds.

2.4. Image reconstructions

Following acquisition of the SDCT and LDCT, projection data was de-identified and exported offline for image reconstruction. Images were reconstructed at 5 mm section thickness with 5 mm section overlap. Both SDCT and LDCT data were reconstructed to obtain conventional FBP images (SD-FBP and LD-FBP) and FIRST images at standard (SD-STD and LD-STD) and strong (SD-STR and LD-STR) strengths. The approximate time for reconstructing FIRST images varied between 5–7 minutes. Mean HU and image noise (standard deviation of mean HU) were recorded by drawing a region of interest (1–1.5cm²) each on right hepatic lobe and main portal vein. These values were used to calculate signal-to-noise (SNR) and contrast-to-noise (CNR) ratios were calculated (Figs. 1–3).

2.5. Qualitative assessment

All de-identified SDCT ($n = 37 \times 3 = 111$) and LDCT ($n = 37 \times 3 = 111$) were viewed on a standalone image viewing software (ClearCanvas workstation, ClearCanvas Inc., Toronto, Canada). Images were assessed in soft tissue window settings (window level = 40, window width = 400); the radiologists were permitted to adjust window settings according to their preference. Two radiologists (RS with 6 years and RDK with 4 years of experience) independently assessed all six CT image series. For each patient, a single image series was displayed at a time. The LDCT images series were displayed prior to the SDCT image series. The interpreting radiologists did not take part in patient recruitment, scanning, data de-identification, or image reconstruction. Each image series was separately evaluated for lesion detection, conspicuity, size, and number.

2.6. Statistical analysis

Data were recorded and analyzed in Microsoft EXCEL (Microsoft Inc., Redmond, Wash.). Mean and standard deviations were calculated for the dose descriptors (CTDIvol and DLP). Wilcoxon signed rank and Cohen's kappa tests were performed to compare qualitative evaluation and to assess interobserver agreement. A p-value of ≤ 0.05 was considered statistically significant. For Cohen's Kappa analysis, a kappa of > 0.6 was termed as a good agreement, 0.2–0.4 as fair agreement and < 0.2 as poor agreement.

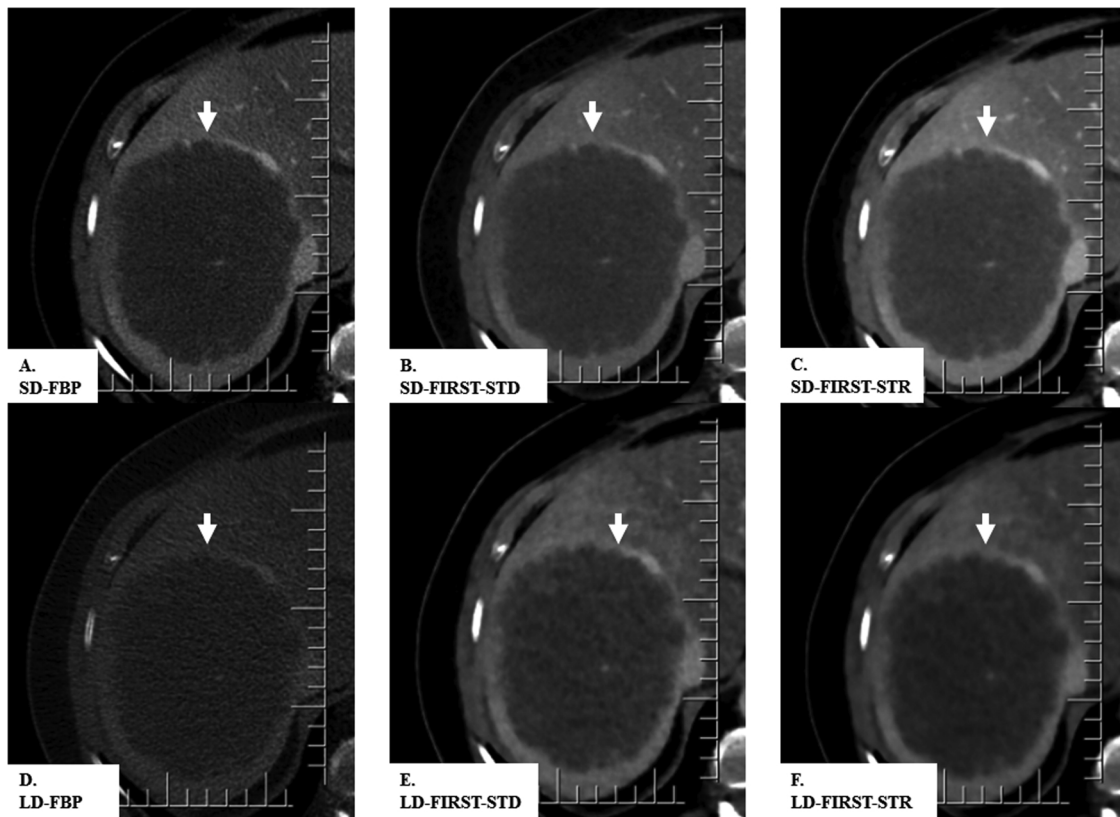


Fig. 1. A 68-year-old woman (BMI 32 kg/m²) underwent contrast-enhanced abdomen CT at SDCT (CTDIvol 22 mGy) and LDCT (2.8 mGy). All SDCT and LDCT images demonstrate a necrotic hepatic lesion (white arrow) in the right hepatic lobe. LD-FIRST images had lower noise and better diagnostic performance than the LD-FBP image.

3. Results

The mean BMI of the recruited patients was 26.2 ± 3 kg/m². None of the patients had metallic hardware within the scanned field of view

of the LDCT. Respective CTDIvol and DLP for the SDCT were 13 ± 4.7 mGy (range, 11–16 mGy) and 549 ± 262 mGy.cm (range, 471–679 mGy.cm). Corresponding values for LDCT were 2.2 ± 0.8 mGy (2–3 mGy) and 49 ± 14 mGy.cm (39–60 mGy.cm),

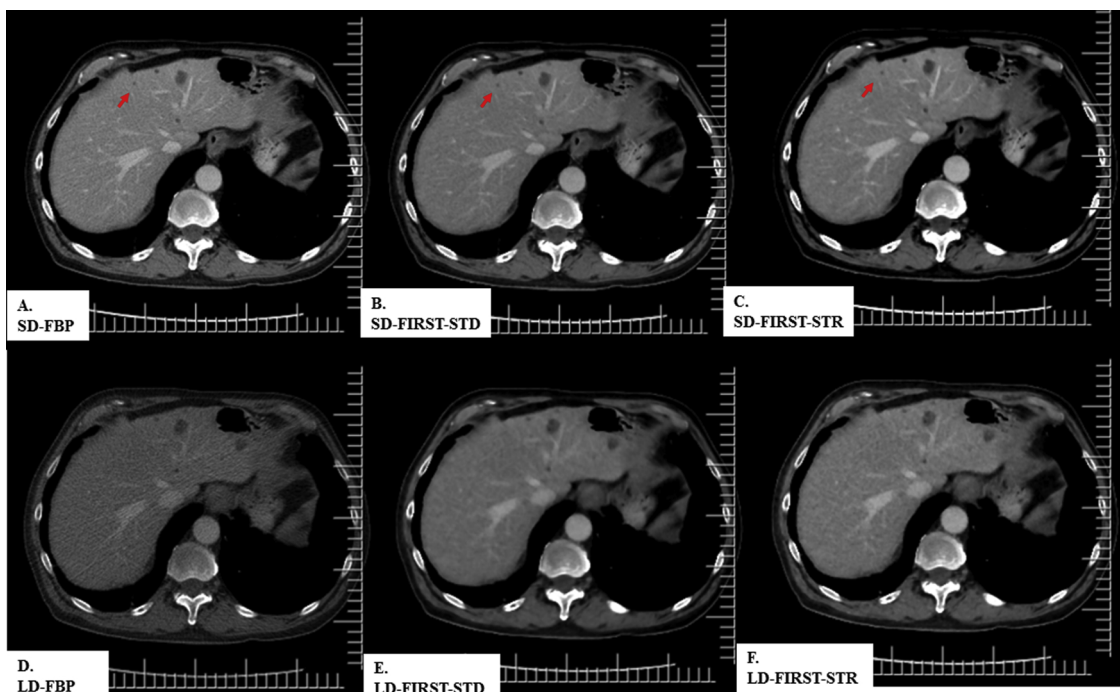


Fig. 2. A 62-year-old man (BMI 23 kg/m²) underwent contrast-enhanced CT of the abdomen at SDCT (CTDIvol 11 mGy) and LDCT (2.8 mGy) images. All SDCT images demonstrate low attenuation hepatic lesions likely cysts in right hepatic lobe. LDCT images detected all lesions except a small cyst (arrow).

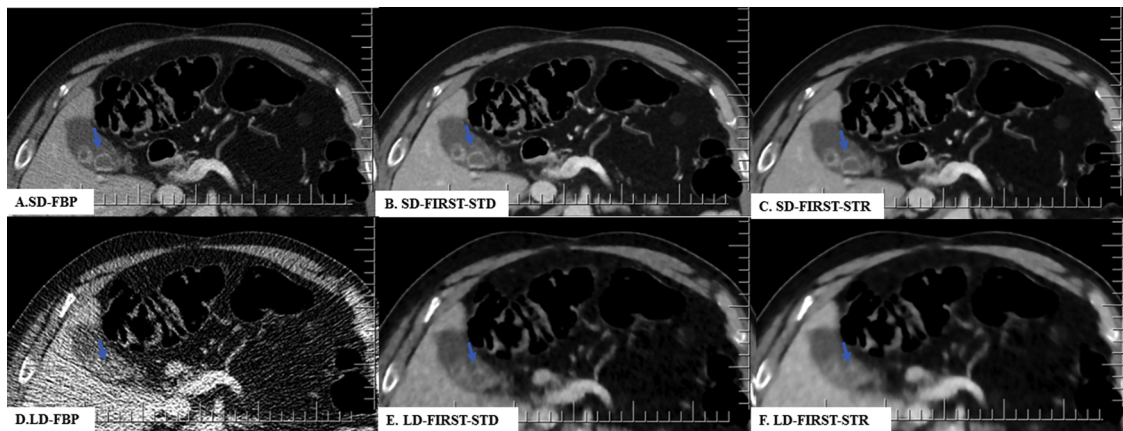


Fig. 3. A 69-year-old man (BMI 31 kg/m²) underwent contrast-enhanced CT of the abdomen at SDCT (CTDIvol 16 mGy) and LDCT (1.7 mGy). All SDCT and LDCT images demonstrated cholelithiasis (arrow). LD-FIRST-STD image had lower noise and better diagnostic performance than the unacceptable LD-FBP image.

Table 1

Mean (± standard deviation) of SNR and CNR for different image reconstruction methods.

Image series	SNR: mean ± standard deviation		CNR: mean ± standard deviation
	Liver	Portal Vein	
SD-FBP	9 ± 2	11 ± 3	3 ± 3
LD-FBP	10 ± 3	13 ± 4	4 ± 3
LD-FIRST-STD	2 ± 1	2 ± 0.7	0.4 ± 0.5
LD-FIRST-STR	16 ± 5	20 ± 7	5 ± 3

respectively. There was a significant statistical difference between the dose descriptors for the SDCT and LDCT ($p < 0.0001$). The SNR and CNR are summarized in [Table 1](#).

There were no differences between the number and types of lesions detected on the SD-FBP and both the SD-FIRST series ($p > 0.9$) (Fig. 1–3). The average lesion size was 13 ± 10 mm (range = 3–32 mm). Both radiologists detected 55 lesions on the SDCT images which included low attenuation liver lesions ($n = 23$), renal cysts ($n = 17$), adrenal nodules ($n = 6$), low attenuation lesions in the pancreas ($n = 4$), cholelithiasis ($n = 2$), retroperitoneal fat stranding with thickening ($n = 1$), ascites with mesenteric fat stranding ($n = 1$), and retroperitoneal lymphadenopathy ($n = 1$).

On the LD-FBP images, the radiologist 1 (R1) detected 39 lesions that included low attenuation liver lesions ($n = 13$), renal cysts ($n = 16$), adrenal nodules ($n = 5$), low attenuation lesions in the pancreas ($n = 1$), cholelithiasis ($n = 1$), retroperitoneal fat stranding with thickening ($n = 1$), ascites with mesenteric fat stranding ($n = 1$), and retroperitoneal lymphadenopathy ($n = 1$). On these images, the radiologist 2 (R2) detected 35 lesions that included low attenuation liver lesions ($n = 13$), renal cysts ($n = 12$), adrenal nodules ($n = 4$), low attenuation lesions in the pancreas ($n = 3$), cholelithiasis ($n = 2$), and retroperitoneal lymphadenopathy ($n = 1$).

Both radiologists detected additional lesions on the LD-FIRST-STD images that were not documented for the LD-FBP images. These included lesions that included low attenuation liver lesions ($n = 2–4$), adrenal nodule ($n = 1$), low attenuation lesions in the pancreas ($n = 2$), cholelithiasis ($n = 1$), retroperitoneal fat stranding with thickening ($n = 1$), and ascites with mesenteric fat stranding ($n = 1$). Patients (BMI > 25.8 kg/m²) with missed lesions on the LD-FIRST-STD images relative to the SDCT images were larger than the patients without missed lesions ($p = 0.01$).

All lesions on LD-FBP images were also seen on the LD-FIRST-STD and STR settings. However, radiologists could not detect three lesions on the LD-FIRST-STR that were seen on the LD-FIRST-STD; these

Table 2

Number of lesions detected by each radiologist on SDCT and different LDCT image series.

Image reconstruction methods	R1 (number of detected lesions)	R2 (number of detected lesions)
SD-FBP	55	55
LD-FBP	39	35
LD-FIRST-STD	49	43
LD-FIRST-STR	46	40

included low attenuation liver lesion ($n = 1$), low attenuation lesions in the pancreas ($n = 1$), cholelithiasis ($n = 1$), and adrenal nodule. [Table 2](#) summarizes the lesion detection by each radiologist.

The number of lesions detected on different SDCT image series were identical.

There were no major artifacts on any of the SDCT or LDCT image series regardless of the reconstruction technique. The inter-observer agreement (kappa-value) were 0.98 and 0.84 for LD-FIRSTSTD and STR levels, respectively.

4. Discussion

FIRST algorithm has been evaluated for radiation dose reduction in patients with lung nodules [14,17] and those undergoing CT angiography of the abdomen [12] or coronary arteries [13,18–20]. Our radiation doses (2.2 ± 0.8 mGy) were substantially lower than the prior abdominal CT angiography study with FIRST (7 ± 2.8 mGy) [12]. Despite the differences in radiation doses between our study and that of Wu et al [12], we noticed an improved lesion detection with the LD-FIRST images as compared to the LD-FBP images. Both radiologists detected more lesions on LD-FIRST images than on LD-FBP images. The additional lesions on the LD-FIRST images included additional liver, adrenal and pancreatic lesions. Both radiologists preferred LD-FIRST images at standard strength over the strong setting since the latter images were “too smooth” for evaluation of major organs such as the liver, pancreas, and kidneys. Other studies have also reported the “too smooth” appearance with different IR techniques at higher strengths of noise reduction [16].

Previous studies have described use of IR techniques to enable radiation dose reduction below 1 mSv for abdomen CT [21–26]. However, most successful studies with sub-mSv radiation doses using IR techniques were performed for evaluation of kidney stones and CT colonography [22–26]. Kidney stones are high contrast findings are not as much affected by high image noise at sub-mSv radiation doses [22]. Air filled lumen also provides a much higher contrast to the colonic wall and polyps, which enables uncompromised evaluation at sub-mSv

[25,26]. Conversely, routine abdomen CT is a more commonly performed procedure which entails evaluation of low-contrast solid organs and lesions in the liver, pancreas, and kidneys. In 2012, Padole et al reported that IR techniques from four different CT vendors (other than the vendor assessed in our study) could not provide acceptable image quality in non-obese patients undergoing sub-mSv routine abdomen CT [21]. Although LD-FIRST images outperformed LD-FBP in terms of lesion detection, both radiologists missed several lesions on both LD-FBP and FIRST images they reported on SDCT images series. However, in contradiction to prior studies, there were no lesions on the sub-mSv abdomen CT images reconstructed with FIRST in patients with BMI $\leq 25.8 \text{ kg/m}^2$. Interestingly, O'Neill et al have also reported that sub-mSv abdomen CT images reconstructed with ASIR technique enabled diagnostic interpretation in non-obese patients with a BMI $< 25.2 \text{ kg/m}^2$ [26]. The study tested visibility of only bowel findings related to Crohn's disease on LDCT of the abdomen [26] as opposed the smaller and lower contrast lesions on our study at similar radiation doses.

Implications of our study include feasibility of deploying sub-mSv routine abdomen CT protocol with FIRST in non-obese, non-overweight patients with BMI $\leq 25.8 \text{ kg/m}^2$. When using FIRST technique for image reconstruction, a standard setting provides better lesion delineation and retention of image texture as opposed to the strong setting. In overweight patients (BMI $> 25.8 \text{ kg/m}^2$), sub-mSv CT for routine abdomen is not possible with the FBP or the FIRST. Missed lesions at sub-mSv CT include liver metastases and pancreatic lesions which have serious diagnostic implications. Future sub-mSv studies should target high contrast situations in the abdomen for evaluation of abdominal vasculature, colonography and kidney stones.

Our study has limitations. Because of the prospective nature of our study, associated additional radiation dose from acquisition of LDCT image series, and stringent inclusion and exclusion criteria, our study sample size is not large ($n = 37$ patients). We did not perform quantitative assessment of FBP or FIRST images since the conventional parameters such as image noise (standard deviation of CT numbers), signal-to-noise ratio, and contrast-to-noise ratio, do not provide an accurate assessment of image quality or diagnostic acceptability of iterative reconstruction techniques. As expected from any CT examination with two or more post-contrast acquisition, there was a short delay between the acquisition of SDCT and LDCT images. We addressed this limitation with planning of LDCT image series before acquisition of SDCT. Due to the portal venous scanning for the SDCT and LDCT image series, the minimal time difference (up to 10 s) did not have a noticeable effect on the evaluation of these two series.

We excluded obese patients since LDCT images for routine abdomen in such patients were unlikely to attain the required diagnostic performance with either FBP or FIRST reconstruction techniques. Suboptimal performance of both FBP and FIRST images in the larger patients included in our study confirmed our decision. Our study focused on routine abdomen protocol for LDCT, and therefore, our results should not apply to other abdominal CT protocols where radiation doses are lower than for routine abdomen CT. For example, abdominal CT for renal colic and colonography are performed at a lower dose than routine abdomen CT. Also, it is unlikely that radiation doses (CTDIvol $2.2 \pm 0.4 \text{ mGy}$) used in our study can provide sufficient information for liver and pancreatic protocols where a preponderance of low-contrast lesions require lower noise and better image quality than needed for the routine abdomen CT images. Another limitation of our study pertains to the use of fixed tube current for acquiring LDCT images as opposed to automatic exposure control for the SDCT images. We used fixed tube current for LDCT because it is easy to apply to reach a targeted radiation dose (DLP 65 mGy.cm ; estimated effective dose just under 1 mSv). Also, because for such LDCT the tube current with automatic exposure control over a short length of acquisition in the upper abdomen will not change substantially from slice to slice or within each slice depending on the patient size.

In summary, recently introduced forward-projected, model-based

reconstruction technique (FIRST) enabled optimal lesion detection in routine abdomen CT at less than 1 mSv radiation dose in patients with body mass less than $\leq 25.8 \text{ kg/m}^2$. The standard setting of FIRST outperforms stronger setting in terms of lesion detection and image texture. Compared to our standard of care, routine abdomen CT protocol, the assessed low dose CT FIRST images can enable a radiation dose reduction of up to 85%.

Conflict of interest

A study coauthor, MKK received research grants from Canon Medical Systems USA, Inc. and Siemens Healthineers. YH and EA are employees of Canon Medical Systems USA, Inc. All study coauthors had unrestricted access to the study data and the manuscript.

Acknowledgments

MKK received research grants from Canon Medical Systems USA, Inc. and Siemens Healthineers. The funding source was Canon Medical Systems, USA Inc., Tustin, California, USA. Grant ID is 226077.

References

- [1] L.L. Geyer, U.J. Schoepf, F.G. Meinel, et al., State of the art: iterative CT reconstruction techniques, *Radiology* 276 (2) (2015) 339–357.
- [2] J. Ambrose, Computerized transverse axial scanning (tomography). II. Clinical application, *Br. J. Radiol.* 46 (552) (1973) 1023–1047.
- [3] A. Laqmani, J.H. Buhk, F.O. Henes, et al., Impact of a 4th generation iterative reconstruction technique on image quality in low-dose computed tomography of the chest in immunocompromised patients, *Rofo* 185 (8) (2013) 749–757.
- [4] J. Hsieh, Adaptive statistical iterative reconstruction: GE white paper, Waukesha, Wis: GE Healthcare, 2008.
- [5] L. Liu, Model-based iterative reconstruction: a promising algorithm for today's computed tomography imaging, *J. Med. Imaging Radiat. Sci.* 45 (2014) 131–136.
- [6] S. Bulla, P. Blanke, F. Hassepass, et al., Reducing the radiation dose for low-dose CT of the paranasal sinuses using iterative reconstruction: feasibility and image quality, *Eur. J. Radiol.* 81 (9) (2012) 2246–2250.
- [7] K. Jensen, A.C. Martinsen, A. Tingberg, T.M. Aalokken, E. Fosse, Comparing five different iterative reconstruction algorithms for computed tomography in an ROC study, *Eur. Radiol.* 24 (12) (2014) 2989–3002.
- [8] Z. Yu, J.B. Thibault, C.A. Bouman, K.D. Sauer, J. Hsieh, Fast model-based X-ray CT reconstruction using spatially nonhomogeneous ICD optimization, *IEEE Trans. Image Proc.* 20 (1) (2011) 161–175.
- [9] J.B. Thibault, K.D. Sauer, C.A. Bouman, J. Hsieh, A three-dimensional statistical approach to improved image quality for multislice helical CT, *Med. Phys.* 34 (11) (2007) 4526–4544.
- [10] S.B. Nam, D.W. Jeong, K.S. Choo, et al., Image quality of CT angiography in young children with congenital heart disease: a comparison between the sinogram-affirmed iterative reconstruction (SAFIRE) and advanced modelled iterative reconstruction (ADMIRE) algorithms, *Clin. Radiol.* 72 (12) (2017) 1060–1065.
- [11] R. Wu, M. Hori, H. Onishi, et al., Effects of reconstruction technique on the quality of abdominal CT angiography: a comparison between forward projected model-based iterative reconstruction solution (FIRST) and conventional reconstruction methods, *Eur. J. Radiol.* 106 (2018) 100–105.
- [12] C. Hassani, A. Ronco, A.E. Prosper, et al., Forward-projected model-based iterative reconstruction in screening low-dose chest CT: comparison with adaptive iterative dose reduction 3D, *Am J Roentgenol.* 211 (3) (2018) 548–556.
- [13] E. Maeda, N. Tomizawa, S. Kanno, et al., The feasibility of Forward-projected model-based Iterative Reconstruction Solution (FIRST) for coronary 320-row computed tomography angiography: a pilot study, *J. Cardiovasc. Comput. Tomogr.* 11 (1) (2017) 40–45.
- [14] Y. Nomura, T. Higaki, M. Fujita, et al., Effects of iterative reconstruction algorithms on computer-assisted detection (CAD) software for lung nodules in ultra-low-dose CT for lung cancer screening, *Acad. Radiol.* 24 (2) (2017) 124–130.
- [15] R. Gnannt, A. Winklehner, D. Eberli, A. Knuth, T. Frauenfelder, H. Alkadhi, Automated tube potential selection for standard chest and abdominal CT in follow-up patients with testicular cancer: comparison with fixed tube potential, *Eur. Radiol.* 22 (September 9) (2012) 1937–1945.
- [16] A. Padole, N. Sainani, D. Lira, et al., Assessment of sub-milli-sievert abdominal computed tomography with iterative reconstruction techniques of different vendors, *World J. Radiol.* 8 (6) (2016) 618–627.
- [17] Y. Funama, D. Utsunomiya, K. Hirata, et al., Improved estimation of coronary plaque and luminal attenuation using a vendor-specific model-based iterative reconstruction algorithm in contrast-enhanced CT coronary angiography, *Acad. Radiol.* 24 (9) (2017) 1070–1078.
- [18] K. Hirata, D. Utsunomiya, M. Kidoh, et al., Tradeoff between noise reduction and artificial visualization in a model-based iterative reconstruction algorithm on coronary computed tomography angiography, *Bull. Sch. Med. Md* 97 (20) (2018) e10810.

- [19] S. Maruyama, Y. Fukushima, Y. Miyamae, K. Koizumi, Usefulness of model-based iterative reconstruction in semi-automatic volumetry for ground-glass nodules at ultra-low-dose CT: a phantom study, *Radiol. Phys. Technol.* 11 (2) (2018) 235–241.
- [20] M.K. Kalra, M. Woisetschläger, N. Dahlström, et al., Radiation dose reduction with Sinogram Affirmed Iterative Reconstruction technique for abdominal computed tomography, *J. Comput. Assist. Tomogr.* 36 (3) (2012) 339–346.
- [21] J.H. Ahn, S.H. Kim, S.J. Kim, I.C. Nam, S.J. Lee, S.Y. Pak, Diagnostic performance of advanced modeled iterative reconstruction applied images for detecting urinary stones on submillisievert low-dose computed tomography, *Acta radiol.* 59 (8) (2018) 1002–1009.
- [22] B.D. Pooler, M.G. Lubner, D.H. Kim, et al., Prospective trial of the detection of urolithiasis on ultralow dose (sub mSv) noncontrast computerized tomography: direct comparison against routine low dose reference standard, *J. Urol.* 192 (5) (2014) 1433–1439.
- [23] L. Lambert, P. Ourednicek, J. Briza, et al., Sub-millisievert ultralow-dose CT colonography with iterative model reconstruction technique, *Peer J.* 31 (4) (2016 Mar) e1883.
- [24] H.J. Kang, S.H. Kim, C.I. Shin, et al., Sub-millisievert CT colonography: effect of knowledge-based iterative reconstruction on the detection of colonic polyps, *Eur. Radiol.* 28 (12) (2018) 5258–5266.
- [25] M.G. Lubner, B.D. Pooler, D.R. Kitchin, et al., Sub-millisievert (sub-mSv) CT colonography: a prospective comparison of image quality and polyp conspicuity at reduced-dose versus standard-dose imaging, *Eur. Radiol.* 25 (7) (2015) 2089–2102.
- [26] S.B. O’Neill, P.D. Mc Laughlin, L. Crush, et al., A prospective feasibility study of sub-millisievert abdominopelvic CT using iterative reconstruction in Crohn’s disease, *Eur. Radiol.* 23 (9) (2013) 2503–2512.